Changes in the NMR-Derived Motional Parameters of the Insulin Receptor Substrate 1 Phosphotyrosine Binding Domain upon Binding to an Interleukin 4 Receptor Phosphopeptide

Edward T. Olejniczak, Ming-Ming Zhou, and Stephen W. Fesik*

Pharmaceutical Discovery Division, Abbott Laboratories, Abbott Park, Illinois 60064

Received December 12, 1996; Revised Manuscript Received January 31, 1997[⊗]

ABSTRACT: Proteins recognize ligands by forming specific intermolecular interactions that often involve solvent exposed residues. Changes in the motional properties of these residues upon binding can affect the conformational entropy of the system and thus are related to the energetics of binding. The role that dynamics plays in ligand recognition can be investigated by comparing the motional properties of a free and ligated protein. NMR relaxation studies are well suited for examining changes in dynamics, especially for motions on a nanosecond to picosecond time scale. Recently, we determined the solution structure of the phosphotyrosine binding (PTB) domain of the insulin receptor substrate (IRS-1) complexed to a tyrosine-phosphorylated peptide derived from the interleukin 4 (IL-4) receptor [Zhou *et al.*, (1996) *Nat. Struct. Biol. 3*, 388−393]. The peptide binds tightly to the protein in a surface exposed pocket, resulting in the partial burial of many protein residues. Using NMR relaxation studies, the dynamics of the backbone nitrogens of IRS-1 PTB domain were studied in both the free protein and the protein when complexed to the IL-4 receptor phosphopeptide. The backbone nitrogens of many residues that make important contacts to the ligand are motionally restricted in the free and complexed protein. Additional residues become motionally restricted only after ligand binding, including several residues that do not make any direct contacts with the ligand. These observed changes in the dynamics are compared to structural features of the complex.

Molecular recognition of a ligand by its protein host occurs due to specific intermolecular interactions that form upon binding. These interactions can result in changes in the conformational freedom of the components of the complex. Changes in conformational freedom have consequences for the energetics of binding based on how it affects the conformational entropy of the system. In some cases the binding pocket becomes more rigid upon ligand binding (Akke *et al.*, 1993; Cheng *et al.*, 1994; Nicholson *et al.*, 1992). This incurs an entropic penalty which must be compensated for by other favorable interactions with the ligand. In other cases, an increase in motion on a picosecond to nanosecond time scale has been observed (Farrow *et al.*, 1994; Kay *et al.*, 1996; Yu *et al.*, 1996). This increase in the conformational freedom of the protein upon complex formation is favored entropically but may be indicative of poor shape complementarity between the protein and ligand. A comparison of the dynamics in a free and ligated protein provides information on how motional properties correlate with binding energy and how the dynamics of a protein can be influenced by intermolecular contacts between the ligand and protein.

Recently, we determined the solution structure of the phosphotyrosine binding (PTB)[1] domain of the insulin receptor substrate 1 (IRS-1) complexed to a tyrosine-phosphorylated peptide derived from the IL-4 receptor (Zhou *et al.*, 1996). The phosphopeptide binds to surface-exposed residues and contacts several different segments of the protein's polypeptide chain. The phosphotyrosine is located in a type I β-turn involving the NPApY residues of the peptide and interacts with both Arg 212 and Arg 227 of the protein. The N-terminal residues of the ligand bind in an extended conformation and form an additional strand of the protein's β-sheet. In addition to interstrand hydrogen bonds the peptide binding is stabilized by contacts between Pro (pY-1) and residues in the C-terminal helix and by the interaction of Leu (pY-8) with a hydrophobic patch formed by Trp 237 and Phe 222 of the protein. These structural features have also been observed in an X-ray crystallographic study of a complex between the IRS-1 PTB domain with a peptide derived from the juxtamembrane region of the insulin receptor (Eck *et al.*, 1996). In addition, the structure of free IRS-1 has been determined by X-ray crystallography and was found to be very similar to the ligated protein (Eck *et al.*, 1996). However, several regions that are disordered in the free protein were found to become ordered in the complex.

Here we report NMR studies on the free and ligated IRS-1 PTB domain to further investigate the changes in the protein that occur upon phosphopeptide binding in solution. Using ^{15}N relaxation studies, differences in the dynamics of the free and complexed protein are quantitated and analyzed using the model-free approach (Lipari & Szabo, 1992). The motional properties revealed by this analysis are compared to structural features of the complex to determine whether motions on this time scale are consistent with the protein−peptide interactions that have been observed (Zhou *et al.*, 1996; Eck *et al.*, 1996).

MATERIALS AND METHODS

NMR Sample Preparation. The PTB domain of IRS-1 (residues 157−267) was cloned, expressed, and purified as

[⊗] Abstract published in *Advance ACS Abstracts,* March 15, 1997.

[1] Abbreviations: NMR, nuclear magnetic resonance; PTB, phosphotyrosine binding; IRS-1, insulin receptor substrate 1; IL-4, interleukin 4; TOCSY, total correlation spectroscopy; NOE, nuclear Overhauser effect; rmsd, root mean square deviation.

S0006-2960(96)03050-4 CCC: $14.00

previously described (Zhou *et al.*, 1996). ^{15}N-Labeled protein was overexpressed in bacteria and grown in a minimal medium containing $^{15}NH_4Cl$. The tyrosine-phosphorylated peptide derived from the IL-4 receptor (LVIAGNPApYRS) was synthesized and purified as described earlier (Piccione *et al.*, 1993). The NMR samples contained 1 mM protein and peptide, in a Tris perdeuterated buffered H_2O/D_2O (9/1) solution (50 mM, pH 6.5) with 50 mM NaCl and 5 mM perdeuterated DTT.

NMR Spectroscopy. NMR spectra were acquired at 30 °C on a Bruker DMX500 or AMX600 NMR spectrometer and processed using in-house written software. The H^N and ^{15}N resonances of the amides in the complex were assigned using triple resonance and isotope-edited NMR experiments as previously described (Zhou *et al.*, 1996). The H^N and ^{15}N resonances of the free protein were assigned using ^{15}N-edited TOCSY and NOE experiments. ^{15}N T_1 and T_2 experiments were recorded with sensitivity-enhanced pulse sequences (Stone *et al.*, 1992; Farrow *et al.*, 1994). The NOE experiments were performed using water flip-back pulses for minimum water saturation and employed gradients for coherence selection (Farrow *et al.*, 1994). The spectra were acquired using recycle delays of 3.5 s between scans for the T_1 and T_2 experiments and 5.5 s for the NOE experiments. These recycle delays are sufficient for recovery of the ^{1}H and ^{15}N magnetization between scans.

Analysis of the Relaxation Data. The T_1 and T_2 relaxation constants were obtained by two-parameter least squares fits of the cross peak heights versus the relaxation delays in the experiments. Nine relaxation delays were used in the fits of the T_1 and T_2 data. Error estimates are based on duplicate relaxation data sets. The steady-state $H^N-^{15}N$ NOE of each residue was calculated as the ratio of the peak height in the spectrum recorded with proton saturation to that observed in a spectrum without proton saturation during the relaxation delay period. Each NOE experiment was run in triplicate from which errors and standard deviations are reported.

The ^{15}N spin relaxation can be expressed in terms of the spectral density functions as

$$\frac{1}{T_1} = \frac{d^2}{4}[3J(\omega_N) + J(\omega_H - \omega_N) + 6J(\omega_H + \omega_N)] + c^2 J(\omega_N) \quad (1)$$

$$\frac{1}{T_2} = \frac{d^2}{8}[4J(0) + 3J(\omega_N) + J(\omega_H - \omega_N) + 6J(\omega_H) + 6J(\omega_H + \omega_N)] + c^2[4J(0) + 3J(\omega_N)] + R_{ex} \quad (2)$$

$$\mathrm{NOE} = 1 + \frac{d^2}{4} T_1 \frac{\gamma_H}{\gamma_N}[6J(\omega_H + \omega_N) - J(\omega_H - \omega_N)] \quad (3)$$

in which $d = (h/2\pi)(\mu/4\pi)\gamma_H\gamma_N(r^{-3})$ and $c = (1/3)^{1/2}\omega_N(\sigma_{||} - \sigma_\perp)$ (Abragam, 1961). An additional term, R_{ex}, was included into the relaxation rate T_2 to take into account the effects of internal motions on a slower time scale which can contribute to chemical exchange broadening (Stone *et al.*, 1992).

The relaxation rates were interpreted using the model-free approach (Lipari & Szabo, 1992). In this approach, the rate and amplitude of internal motions for individual H^N-N vectors are described in terms of a generalized order parameter (S^2), an overall rotational correlation time of the molecule (τ_m), and an effective correlation time for fast internal motions (τ_e). This approach assumes a spectral density function $J(\omega)$ of the form

$$J(\omega) = \frac{2}{5}\left[\frac{S^2\tau_m}{1 + (\omega\tau_m)^2} + \frac{(1 - S^2)\tau}{1 + (\omega\tau)^2}\right] \quad (4)$$

where $1/\tau = 1/\tau_m + 1/\tau_e$.

The model-free parameters were obtained by using the expressions given in eqs 1−3 and the spectral density function defined in eq 4 to find a consistent set of parameters that minimize the rmsd error between the predicted and the experimentally measured T_1, T_2, and NOE values. The overall rotational correlation time τ_m was initially estimated from T_1/T_2 ratios of well-resolved peaks corresponding to the amides of residues located in elements of regular secondary structure (Kay *et al.*, 1993). The minimization procedure that was used is based on protocols described earlier (Stone *et al.*, 1992). The uncertainties in the model-free parameters were estimated by performing Monte Carlo simulations using the uncertainties in the measured relaxation rates (Palmer *et al.*, 1991).

Contributions to R_{ex} expected from the observed chemical shift changes of the amides between the free and complexed protein were simulated by solving the coupled differential equations of the form (Mehring, 1983)

$$\mathrm{d[M]}/\mathrm{d}t = [i\omega + \pi][\mathrm{M}]$$

$$[i\omega + \pi] = \begin{bmatrix} \omega_{on} + \frac{i}{T_2} - k_{on} & k_{off} \\ k_{on} & \omega_{off} + \frac{i}{T_2} - k_{off} \end{bmatrix} \quad (5)$$

where k_{on} and k_{off} are the on and off rates, respectively, and ω_{on} and ω_{off} are the resonance frequencies of the amides in the complex and in the free protein.

The solution takes the form: $[\mathrm{M}] = [\mathrm{s}]\exp[(\lambda)t[\mathrm{s}]^{-1}][\mathrm{P}]$, where [P] is a column vector of equilibrium concentrations of free and bound protein, [s] is the QR transformation matrix, and λ is a column vector of eigenvalues of the matrix $[i\omega + \pi]$. In the simulations, it was assumed that the dipolar contribution to T_2 was the same in the free and complexed protein and that the exchange rates could be estimated by assuming diffusion-controlled binding of the ligand to the surface-exposed binding pocket. This second assumption leads to an estimate for k_{on} of 5×10^9/(mol s) (Fersht, 1977) from which an off rate of 10^3/(mol s) is obtained using the measured dissociation constant ($K_d = 6\ \mu$M). From these equations and parameters estimates of line-width changes are obtained.

Calculation of Surface Area. Solvent-accessible and contact surface areas were calculated with a probe radius of 1.6 Å using the program X-PLOR (Brunger, 1992). The ratio of the calculated surface area in the complex to the surface area of the amino acid in an extended peptide (Chothia, 1975) is reported.

RESULTS AND DISCUSSION

Overview of Relaxation and Motional Parameters. Relaxation rates were obtained from a two-parameter fit to the

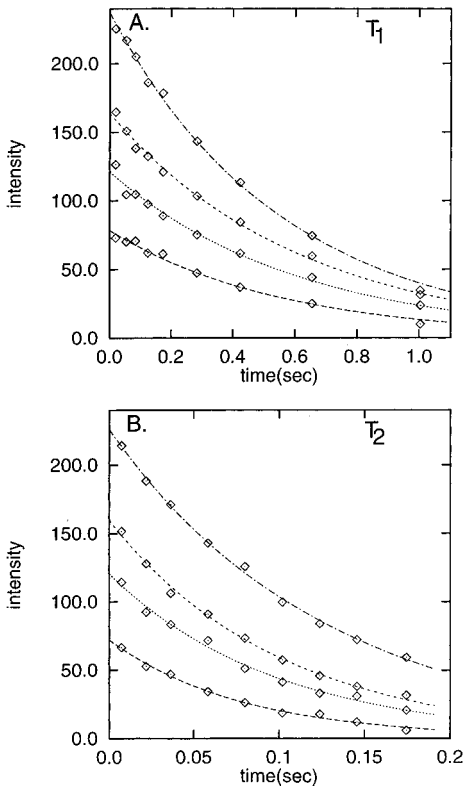

FIGURE 1: Examples of (A) T_1 and (B) T_2 decay curves. The curves from top to bottom are for the relaxation data of Glu 200, Ala 202, Phe 222, and Glu 263 in the complexed protein.

measured longitudinal and transverse relaxation data. Examples of these fits are shown in Figure 1. Peak heights were used in the analysis to minimize problems due to resonance overlap. Resonances with weak intensity due to rapid amide−solvent exchange had the largest errors in the fits. The relaxation data for the free and complexed IRS-1 PTB domain are summarized in Figure 2. The average T_1 in the complexed protein is higher than in the free protein, while the T_2 is smaller. These data are consistent with the slightly higher rotational correlation time calculated for the complex (i.e., 6.8 ± 0.5 ns) compared to the free protein (6.4 ± 0.5 ns). These correlation times are consistent with those obtained for other proteins of similar size (Kay *et al.*, 1996; Yu *et al.*, 1996; Buck *et al.*, 1995; Stone *et al.*, 1992).

The model-free parameters (S^2, τ_e, and R_{ex}) obtained from fits of the relaxation data are shown in Figure 3. The average errors are small, being 4% for the free protein and 3% for the complex. Larger than average errors are observed for residues in the free protein with small order parameters. For most residues, the order parameters (S^2) in the complex and free protein are between 0.7 and 0.9, which indicates that rapid motions on the picosecond time scale are restricted. Exceptions occur for residues in the N- and C-terminus and near loops linking segments of secondary structure.

The secondary structure and solvent accessibilities for the residues of the IRS-1 PTB domain are displayed in Figure 4. No clear trends can be observed between these parameters and the observed S^2 values. For example, amides in defined secondary structure for both the free and complexed protein generally have larger than average S^2 values. However, there are exceptions. Trp 237, for instance, is in an element of regular secondary structure, but in the free protein it has a lower than average order parameter. Similarly, residues 227−231 which are located in the loop between β6 and β7 and are solvent exposed might be expected to have smaller order parameters. However, as shown in Figure 3, these residues have large S^2 values.

Deviations either from the average or between the free and complexed protein's order parameters are shown in Figure 4. Errors in the order parameters are propagated in these differences, leading to larger uncertainties. The average estimated error for the difference is 0.03. However, larger individual errors exist. A qualitative comparison of the data in Figure 4C,D indicates that the complex tends to have a smaller range of order parameters than the free protein. Order parameters which differ from the average in the free protein tend to move toward the average in the complex.

Contributions from R_{ex}. Large values of R_{ex} are generally indicative of line broadening due to chemical exchange (Stone *et al.*, 1992). Assuming exchange between two states, these motions are typically on the millisecond to microsecond time scale (Li & Montelione, 1995). For a complex, the conformational changes that occur in the protein to accommodate the ligand will be modulated at the time scale of the on and off rate of ligand binding. These conformational changes lead to the observed chemical shift differences between the free and bound protein which can result in chemical exchange broadening. The observed effect depends on the magnitude of the chemical shift difference between the free and bound state, the relative concentrations of protein and ligand, and the exchange rates. A qualitative estimate of this contribution to R_{ex} in the complex was made by simulating the chemical exchange effects.

The calculated contribution to R_{ex} from ligand exchange is compared to the observed R_{ex} for the free and complexed protein (Figure 5). The simulations predict a general increase in R_{ex} for the complex (Figure 5C) which is observed experimentally (Figure 5B). However, the predicted increase from this model is only about a third of what is observed experimentally, suggesting that R_{ex} is dominated by other changes in dynamics on different time scales that occur upon ligand binding. This is consistent with the fact that the poorest correlation is for residues Asn 210, Arg 213, Arg 227, and Val 230 which make direct contact to the ligand and are thus expected to have additional changes in their motional properties upon ligand binding.

Mobility in the Free Protein. Several residues that make important contacts with the ligand show large order parameters in the free protein. Two critical residues for binding to the phosphotyrosine of the peptide are Arg 212 and Arg 227 (Figure 6) (Zhou *et al.*, 1996; Eck *et al.*, 1996). Mutation of these two residues results in a total loss of binding (Zhou *et al.*, 1996). The backbone nitrogens for these two residues have large order parameters in both the free protein and the complex. This might be expected for Arg 212 because it lies in a well-defined piece of secondary structure (β5) (Figure 6). However, Arg 227 is located in a large loop. All of the residues in this loop (residues 225−232) have large order parameters for their backbone amides (Figure 3A), indicating limited motions on a nanosecond to picosecond time scale. The side chains of these residues have broader resonances indicative of slower motions.

The residues in the loop that connect β4 and β5 (residues 208−211) also make important contacts with the ligand and have large backbone order parameters in both the free and complexed protein. In the complex, the carbonyl oxygens

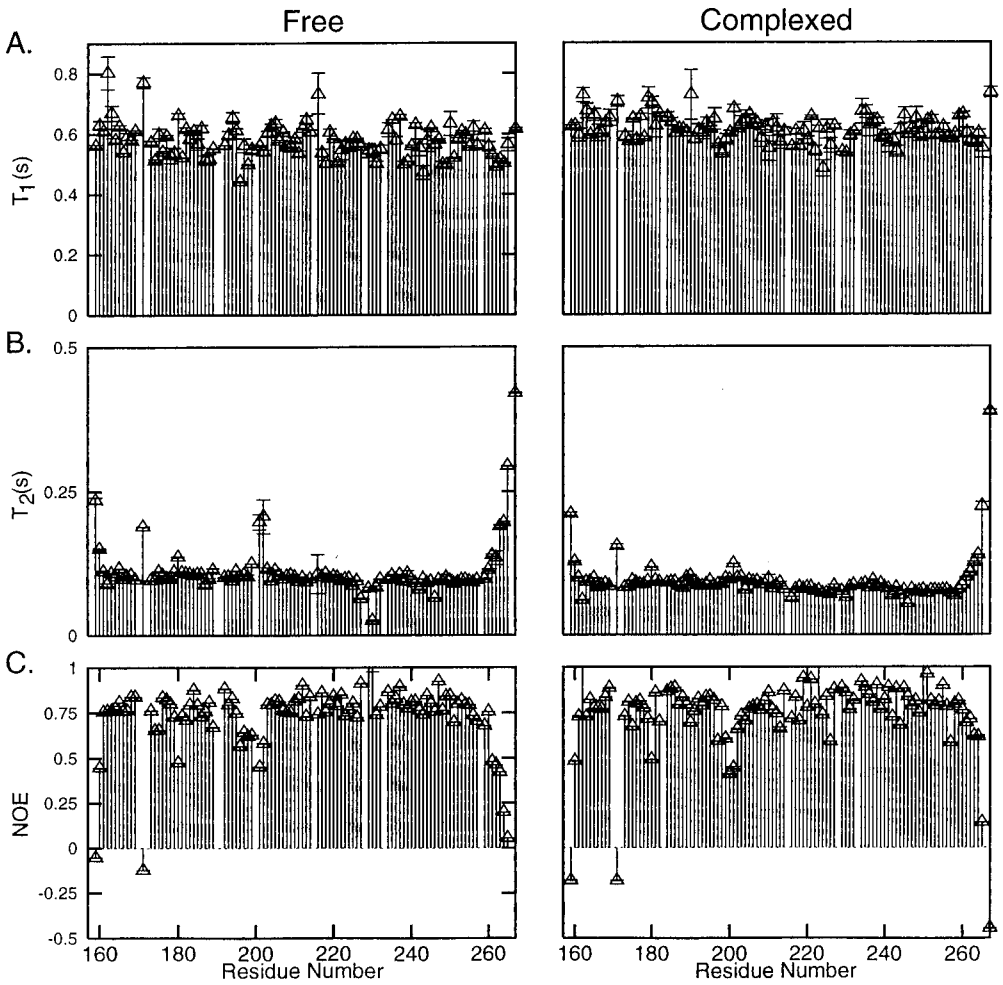

FIGURE 2: Plots of the measured ^{15}N relaxation parameters and their uncertainties as a function of residue number for the free and complexed protein. Residues for which no results are shown correspond to either proline residues or residues for which the H^N resonances were severely overlapped. The plots are from top to bottom (A) T_1, (B) T_2, and (C) the heteronuclear NOE.

of Leu 208 and Ile 211 are within hydrogen-bonding distance of the side chain of Asn (pY-3), the first residue in the NPXpY motif of the ligand. The carbonyl of Met 209 is also in a position to contact the backbone of the ligand at pY-1 (Zhou *et al.*, 1996; Eck *et al.*, 1996). These interactions may facilitate the partial burial of these polar atoms of the ligand. There is evidence that the NPXpY motif of the ligand forms a β-turn when free in solution (Trub *et al.*, 1995). Recognizing this preformed structural motif of the peptide by restricting the mobility of the surface exposed complementary residues in the protein would thus increase the binding affinity for the peptide.

The peptide residues N-terminal to the NPXpY sequence show no signs of preformed structure in solution (data not shown) but upon binding to IRS-1 become an extension to the β-sheet of the protein (Zhou *et al.*, 1996; Eck *et al.*, 1996). The N-terminal hydrophobic residue Leu (pY-8) sits in a pocket formed by residues Phe 222 and Trp 237 of the protein. Contacts between the protein and this hydrophobic residue of the ligand are very important for high-affinity binding (Songyang *et al.*, 1995). The backbone amide of Phe 222 has very little mobility in the free protein or the complex based on its large order parameters.

Several residues that do not directly contact the ligand become more motionally restricted in the complex. In the complex, the reduced mobility of the loop between β3 and β4 is indicated by both an increase in the order parameters and an increase in the effective correlation times of the motions. The residues in this loop do not directly contact any residues of the peptide in the complex. However, they are attached to β2 and β5 through loops that form one side of the ligand binding pocket in the complex (Figure 6). The reduced mobility of β3 and β4 in the complex may therefore be due to indirect contacts with the ligand.

Mobility for Residues in the Protein−Peptide Complex. Trp 237 forms part of the pocket for Leu (pY-8) of the ligand. In the free protein, the order parameters for the backbone ($S^2 = 0.74$) and side chain nitrogens ($S^2 = 0.68$) are smaller than that of Trp 164 [$S^2 = 0.80$ (N), $S^2 = 0.77$ (Nϵ)], which is buried in the protein structure. Trp 237 becomes less exposed to solvent in the complex, resulting in changes in its motional parameters. In the complex, the order parameters are similar to those of the other buried tryptophan residue of the protein.

Another residue which contacts the peptide is His 216. It is located at the end of β5 (Figure 6), and in the free protein its amide is exposed to solvent. In the complex, its amide points toward the backbone of the peptide and is protected from solvent (Zhou *et al.*, 1996). The side chain of His 216 is also close to the side chain of Val (pY-7) of the peptide. Its order parameter is lower than average in the free protein but slightly higher than average in the complex.

In solution, the C-terminal helix is shorter in the free protein compared to this helix in the complex. The shorter

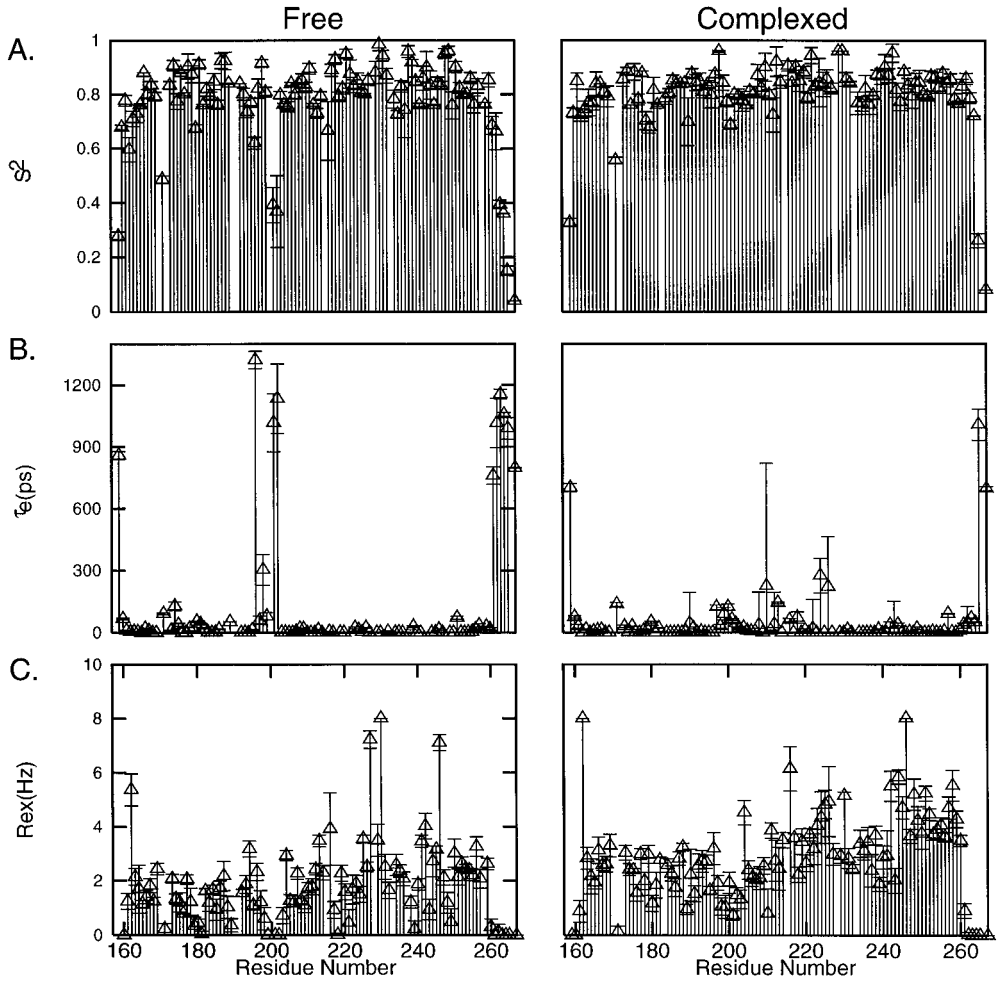

FIGURE 3: Plots of the model-free motional parameters and their uncertainties as a function of residue number for the free and complexed protein. The plots are from top to bottom (A) generalized order parameter S^2, (B) effective correlation time τ_e, and (C) R_{ex} the chemical exchange contribution to T_2.

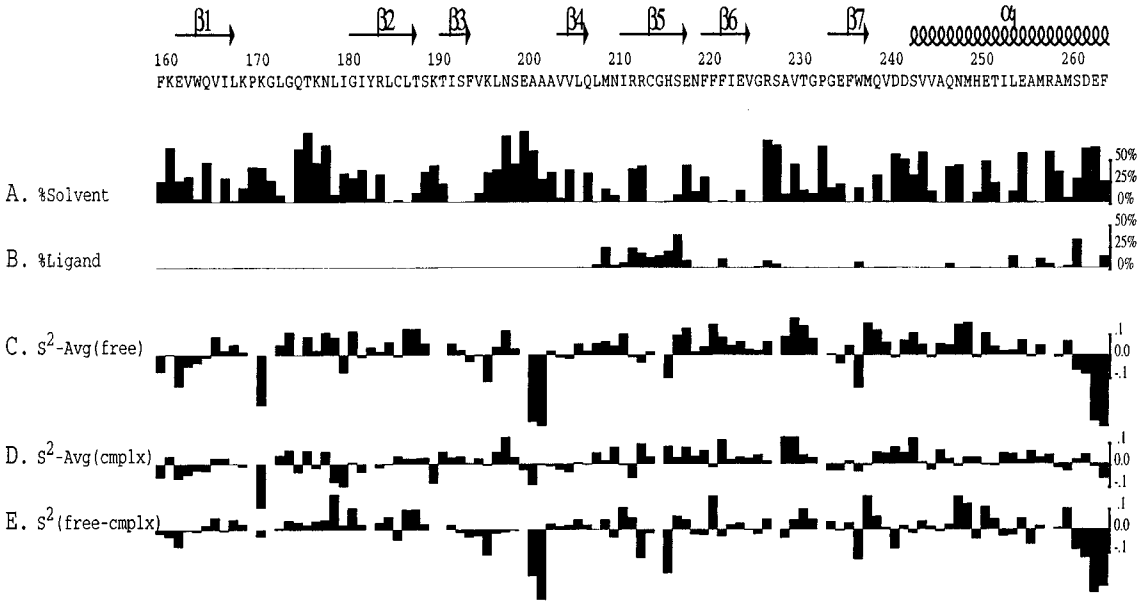

FIGURE 4: Comparison of structural factors: (A) percent of surface area of the amino acid that is solvent exposed, (B) percent of amino acid surface area in contact with ligand, (C) deviation in the measured order parameter, S^2, from the average for the free protein and (D) for the complex, and (E) the difference between S^2 in the free protein and the complex.

helix is reflected in the change in motional parameters of residues 260−264 where a distinct reduction of order parameters is observed in the free protein. In the free protein, the order parameters drop precipitously at residue 260, while in the complex residue 261 shows a larger order parameter with a more gradual decrease between residues 262 and 264. In the complex, Met 260, Met 257, and Leu 254 make contact with the Pro at pY-2 of the ligand (Zhou *et al.*, 1996; Eck *et*

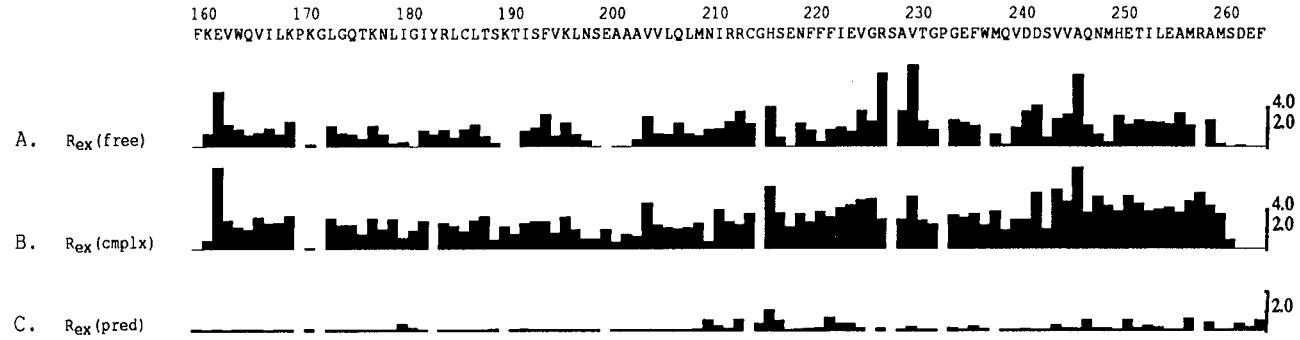

FIGURE 5: Comparison of (A) R_{ex} of free and (B) R_{ex} ligated protein compared to (C) the predicted contribution to R_{ex} from the exchange of ligand on and off the protein.

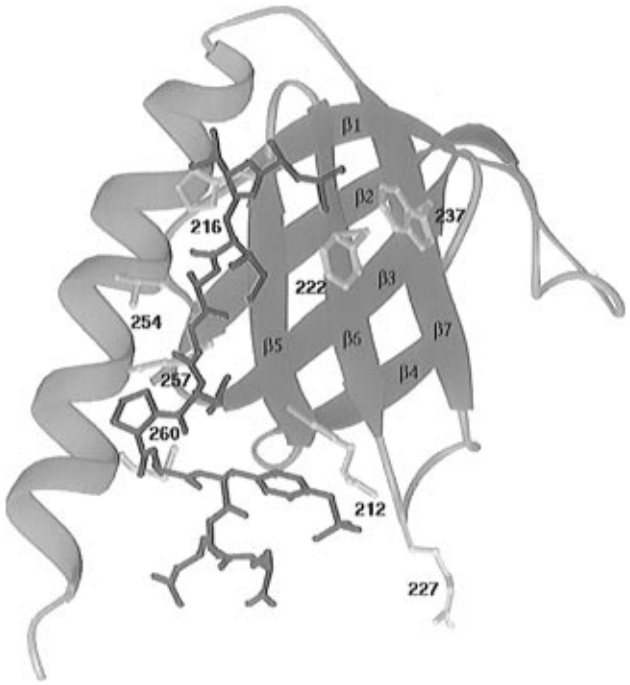

FIGURE 6: Ribbons (Carson, 1987) depiction of the averaged minimized NMR structure of the IRS-1 PTB domain−IL-4 receptor peptide complex with the side chains of residues described in the text displayed.

al., 1996). The two Met residues also contact Ala at (pY-1) of the peptide. These residues form a hydrophobic cluster in the complex with the proline of the ligand at its center (Figure 6). In the absence of a ligand, the hydrophobic residues at the end of the helix would be exposed to solvent. This would be energetically unfavorable and would not be expected to contribute favorably to an extension of this helix.

Comparison to Disordered Regions in the Crystallographic Studies. In the crystal structure of the free protein, several regions are disordered that are better defined in the liganded structure (Eck *et al.*, 1996). These regions are the loop between β3 and β4 and the end of the C-terminal helix. These regions correlate with some of the portions of the protein that change their relaxation properties in solution. The disorder observed in the crystal may therefore be related to motional properties of the free protein. In the crystal structure of the free protein, the residues that form the penultimate turn of the C-terminal helix in the ligated protein are disordered. These residues still maintain some helical character (residues 257−260) in the free protein in solution based on the characteristic NOEs that are observed (data not shown). However, the relaxation parameters (Figure 3) indicate that this is a very flexible region. The last four residues of this helix are not helical and are also very flexible in the free protein.

Comparison of the Changes in Dynamics of the Peptide-Bound Form of IRS-1 PTB and the Phospholipase Cγ1 SH2 Domain. Earlier structural studies have shown that PTB domains bind phosphopeptides in a distinct manner from SH2 domains (Zhou *et al.*, 1995, 1996; Eck *et al.*, 1996). The data presented here indicate that the changes in the dynamics of these proteins upon peptide binding may also be distinctly different. In the SH2 domain of phospholipase Cγ1, no overall change in dynamics was observed for backbone atoms in the peptide-bound form (Farrow *et al.*, 1994). Side chains near to the pTyr binding site were more rigid, but residues that form the hydrophobic binding site for the C-terminal portion of the peptide were mobile in both the free and peptide-bound protein (Kay *et al.*, 1996). In contrast, we find that the backbone atoms of the peptide-bound form of the PTB domain of IRS-1 show less mobility on the picosecond time scale than the free form (Figures 3 and Figure 4). This includes the side chain of Trp 237 which forms part of the hydrophobic binding site for the Leu residue of the peptide at pY-8. Furthermore, the C-terminal helix is extended and becomes less mobile in the peptide-bound form of the protein.

A larger change in the dynamics of IRS-1 upon peptide binding when compared to what is found in SH2 domains is consistent with the structural differences in the binding mode of their peptides. In SH2 domains, the phosphopeptide binds almost perpendicular to the protein's β-sheet while in PTB domains it binds parallel and becomes an extension of the β- sheet (Zhou *et al.*, 1995, 1996). The binding pocket of SH2 domains is also framed by several loops that reduce its exposure when compared to the more open pocket of the IRS-1 PTB domain. These differences in the binding mode are expected to lead to larger changes in solvent exposure and more ligand contacts to backbone amides in IRS-1 than in the SH2 domain of phospholipase Cγ1. These structural features of the peptide binding of IRS-1 correlate with factors that lead to larger order parameters in proteins.

CONCLUSIONS

We have determined and compared the motional parameters for the free and complexed PTB domain of IRS-1 using the model-free formalism. Differences between the measured parameters for the free and complexed protein correlate with residues that make specific contacts to the ligand. Ligand binding resulted in a restriction in motion for several residues that contact the peptide. It was also apparent that several

residues which make contact with the ligand are already motionally restricted in the free protein and that the mobility of their backbone amides does not significantly change after ligand binding.

A study of the motional properties of backbone resonances gives only a partial picture of the dynamic changes that occur upon binding. Most of the contact with the ligand is through side chains for which no information is obtained. Furthermore, the time scale of motions that can be detected by relaxation measurements and those important for ligand recognition may be quite different. Despite these limitations, these data can lead to some insight into the role that dynamics may have on ligand recognition.

ACKNOWLEDGMENT

We thank L. Yu and H. Liang for helpful discussions and assistance in the data analysis and S. Shoelson for supplying the peptide and the DNA construct of the IRS-1 PTB domain used in the studies.

REFERENCES

Abragam, A. (1961) *Principles of Nuclear Magnetism*, Clarendon Press, Oxford.

Akke, M., Skelton, N. J., Kordel, J., Palmer, A. G., III, & Chazin, W. J. (1993) *Biochemistry 32*, 9832−9844.

Brunger, A. T. (1992) *X-PLOR 3.1 Manual*, Yale University Press, New Haven, CT.

Buck, M., Boyd, J., Redfield, C., MacKenzie, D. A., Jeenes, D. J., Archer, D. B., & Dobson, C. M. (1995) *Biochemistry 34*, 4041−4055.

Carson, M. (1987) *J. Mol. Graphics 5*, 103−106.

Cheng, G. W., Lepre, C. A., & Moore, J. M. (1994) *Biochemistry 33*, 4093−4100.

Chothia, C. (1975) *J. Mol. Biol. 105*, 1−14.

Eck, M. J., Dhe-Paganon, S., Trub, T., Nolte, R. T., & Shoelson, S. E. (1996) *Cell 85*, 695−705.

Farrow, N. A., Muhandiram, R., Singer, A. U., Pascal, S. M., Kay, C. M., Gish, G., Shoelson, S. E., Pawson, T., Forman-Kay, J. D., & Kay, L. E. (1994) *Biochemistry 33*, 5984−6003.

Fersht, A. (1977) *Enzyme Structure and Mechanism*, W. H. Freeman and Co., New York.

Kay, L. E., Xu, G.-Y., Singer, A. U., Muhandiram, D. R., & Forman-Kay, J. D. (1993) *J. Magn. Reson. 86*, 110−126.

Kay, L. E., Muhandiram, D. R., Farrow, N. A., Aubin, Y., & Forman-Kay, J. D. (1996) *Biochemistry 35*, 361−368.

Li, Y., & Montelione, G. T. (1995) *Biochemistry 34*, 2408−2423.

Lipari, G., & Szabo, A. (1992) *J. Am. Chem. Soc. 104*, 4546−4559.

Mehring, M. (1983) *Principles of High Resolution NMR in Solids*, Springer-Verlag, New York.

Nicholson, L. K., Kay, L. E., Baldisseri, D. M., Arango, J., Young, P. E., Bax, A., & Torchia, D. A. (1992) *Biochemistry 31*, 5253−5263.

Palmer, A. G. I., Rance, M., & Wright, P. E. (1991) *J. Am. Chem. Soc. 113*, 4371−4380.

Piccione, E., Case, R. D., Domchek, S. M., Hu, P., Chaudhuri, M., Backer, J. M., Schlessinger, J., & Shoelson, S. E. (1993) *Biochemistry 32*, 3197−3202.

Songyang, Z., Margolis, B., Chaudhuri, M., Shoelson, S. E., & Cantley, L. C. (1995) *J. Biol. Chem. 270*, 14863−18466.

Stone, M. J., Fairbrother, W. J., Palmer, A. G. I., Reizer, J., Saier, M. H., & Wright, P. E. (1992) *Biochemistry 31*, 4394−4406.

Trub, T., Choi, W. E., Wolf, G., Ottinger, E., Chen, Y., Weiss, M., & Shoelson, S. E. (1995) *J. Biol. Chem. 270*, 18205−18208.

Yu, L., Chang-Xi, Z., Yuk-Ching, T., & Fesik, S. W. (1996) *Biochemistry 35*, 9661−9666.

Zhou, M.-M., Ravichandran, K. S., Olejniczak, E. T., Petros, A. M., Meadows, R. P., Sattler, M., Harlan, J. E., Wade, W. S., Burakoff, S. J., & Fesik, S. W. (1995) *Nature 378*, 584−592.

Zhou, M.-M., Huang, B., Olejniczak, E. T., Meadows, R. P., Shuker, S. B., Miyazaki, M., Trub, T., Shoelson, S. E., & Fesik, S. W. (1996) *Nat. Struct. Biol. 3*, 388−393.

BI963050I